DOI 10.5012/bkcs.2010.31.04.989

Photophysical and Electrochmical Studies of *N,N*-Bis (2,5-di-*tert*-butylphenyl) - 3,4,9,10 perylenebis (dicarboximide) (DBPI)

Ibrahim S. El-Hallag* and Samy A. El-Daly

*Chemistry Department, Faculty of Science, Tanta University, Tanta 31527, Egypt. *E-mail: ielhallag@yahoo.co.uk*
Received February 12, 2009, Accepted January 6, 2010

The titled dye of DBPI gives amplified spontaneous emission (ASE) with maximum at 580 nm upon pumping by nitrogen laser (λ_{ex} = 337.1 nm). The ground state absorption cross section (σ_A) and emission cross section (σ_E) as well as effective emission cross section(σ^*_E) have been determined. The electronic absorption spectra of DBPI were measured in ethanol and tetrahydrofuran at room and low temperature. DBPI displays molecular aggregation in water. The photochemical reactivity of DBPI was also studied in carbon tetrachloride upon irradiation with 525 nm light. The electrochemical investigation of DBPI dye has been carried out using cyclic voltammetry and convolution deconvolution voltammetry combined with digital simulation technique at a platinum electrode in 0.1 mol/L tetrabutyl ammonium perchlorate (TBAP) in two different solvents acetonitrile (CH_3CN) and dimethylformamide (DMF). The species were reduced *via* consumption of two sequential electrons to form radical anion and dianion (EE mechanism). In switching the potential to positive direction, the compound was oxidized by loss of two sequential electrons, which were followed by a fast dimerization and/or aggregation process i.e $EC_{dim1}EC_{dim2}$ mechanism. The electrode reaction pathway and the chemical and electrochemical parameters of the investigated compound were determined using cyclic and convolutive voltammetry. The extracted electrochemical parameters were verified and confirmed *via* digital simulation method.

Key Words: Perylene derivative, Amplified spontaneous emission, Dimerization, Cyclic voltammetry, Digital simulation

Introduction

The bis(2,5-di-tert-butylphenyl) imide(DBPI) of 3,4,9,10-perylenetetracarboxylic dianhydride is a member of a class of vat dyes that intrinsically are strongly colored and have high fluorescence quantum yield.[1,2] These properties make dyes such as DBPI potentially useful as photo sensitizers in energy and electron transfer reaction [3,4] and in site-selective spectroscopy experiments with biological systems.[5,6] Applications of perylene diimides as laser dyes and in p-n heterojunction solar cells have already been demonstrated by Bird and co-workers.[7]

In order to evaluate the potential usefulness of dyes such as DBPI as photosensitizer, it is necessary to determine their photophysical properties and redox potentials. The bulky *tert*-butyl groups on DBPI dye makes this dye relatively soluble in a number of organic solvents.[8] DBPI dye was first prepared and studied by Rudemacher *et al*.[9] and its large scale synthesis was more described by Langhals.[10] The commercial product was probably a mixture of cis and trans a tropic isomers, whose spectral properties are very similar.[10] In addition to fluorescence properties of DBPI in solid state, kinetic and energetic properties of the singlet and triplet excited states have been examined.[11]

In previous papers,[12-16] certain photophysical characteristics of DBPI have been reported e. g. a fluorescence quantum yield of unity, high photostability, energy transfer from certain blue laser dyes, fluorescence quenching by cobalt ions and molecular oxygen as well as the effect of re-absorption on fluorescence lifetime has also been studied. In this article we report the electronic absorption spectrum at room and low temperature, amplified spontaneous emission, photoreactivity in carbon tetrachloride of DBPI.

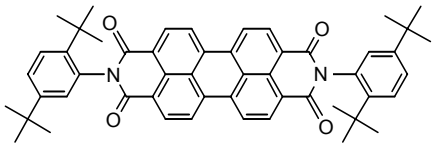

DBPI

To the best of our knowledge of literature there is no report on the electrochemistry of DBPI *via* cyclic voltammetry and convolution-deconvolution transforms. So, in the present manuscript we investigated the photophysical properties and the electrochemical behaviour of DBPI dye using cyclic voltammetry and convolution-deconvolution transforms. The experimental chemical and electrochemical parameters were confirmed and verified *via* digital simulation method.

Experimental

DBPI (Aldrich) was dissolved in a minimum volume of chloroform; the dye was precipitated by adding methanol. The precipitate was collected by filtration and dried in vacuum. All solvents used in this work were of spectroscopic grade.

Low temperature electronic absorption spectra were taken on a shimadzu double beam spectrophotometer UV-200 connected with cooling unit (DN 1704 variable temperature liquid nitrogen cryostat) oxford instruments. UV-visible absorption spectra were measured using a Shimadzu UV-1200S spectrophotometer. Fluorescence lifetime were measured by the single photon counting technique using an air flash lamp operating between 20 and 40 KHz. Excitation wavelengths were selected using a band-pass filter, the emission wavelengths were selected

by appropriate filter (Schott, Mainz, Germany). The data were registered in a 1000 channels analyzer with a resolution of 24 channels/ns. The decay profiles were analyzed by iterative convolution using autocorrelation and residual criteria.[17] Amplified spontaneous emission (ASE) was measured using a nitrogen laser (type 1 M 50 A Lambda physics, λ_{ex} = 337.1 nm, pulse duration = 5 ns) as excitation source and an optical multichannel analyzer (type OMA II. Princeton Applied Research Corp.) as detector.[18] The dye cuvett was placed in the focus of a cylinder lens, which concentrate the nitrogen laser beam to a narrow line. The dye concentration was 5×10^{-5} M in DMF. Eight ASE spectra were recorded for different pulse energies between 0.1 and 1.5 mJ. All spectra were measured in the unsaturated light amplification region. Within the model used,[18] the relation between ASE intensity I and excitation pulse intensity P is given by equations 1-3.

$$I(L,\lambda,p) = F(\lambda)N_1(p) \int_0^l \exp[N_1(p)\sigma^*_E(\lambda) - N_0(p)\sigma_A(\lambda)]dx \quad (1)$$

$$N_1 = N \frac{\sigma_{ex}k_\tau p}{\sigma_{ex}k_\tau p + \frac{1}{\tau}} \quad (2)$$

$$N = N_o + N_1 \quad (3)$$

Where N are the total dye concentration in molecules/cm^3, N_o and N_1 are the populations of the ground state (s_o) and the excited state (s_1) respectively, σ_A is the absorption cross section of the s_o, σ_{ex} is σ_A at 337.1 nm., σ^*_E is the effective emission cross section. L is the length of the excited region within the cuvette (16 - 19 mm), τ is the lifetime of s_1 state, k_τ is a correction factor and F is a factor depending on fluorescence intensity, detector sensitivity and geometrical conditions. The factor k_τ gives state conditions and depends on the ratio of excitation pulse duration to s_1 lifetime (τ). The difference between emission cross section σ_E and effective emission cross section σ^*_E we interpret as the absorption cross sections σ^*_A of $s_1 \rightarrow s_n$ transitions. F as well as σ^*_E are determined from the ASE spectra by curve fitting. The emission cross section σ_E is calculated from equation(4), where E means the normalized fluorescence line shape function, which is correlated with fluorescence quantum yield ϕ_f by equation(5).

$$\sigma_E(\lambda) = \frac{E(\lambda)\lambda^4}{8\pi\tau c n^2} \quad (4)$$

$$\int E(\lambda)\, d\lambda = \phi_f \quad (5)$$

Where n is the refractive index of the dye solution, c is the velocity of light in vacuum, E (λ) is obtained from solutions whose absorptivities are low to avoid reabsorption processes (optical density at absorption maximum $\leq$ 0.1). The excited state absorption cross-section σ^*_A is calculated from the difference ($\sigma_E - \sigma^*_E$).[18] Absolute light intensities were measured using ferrioxalate actinometry as described by Hatcher and Parker.[19,20]

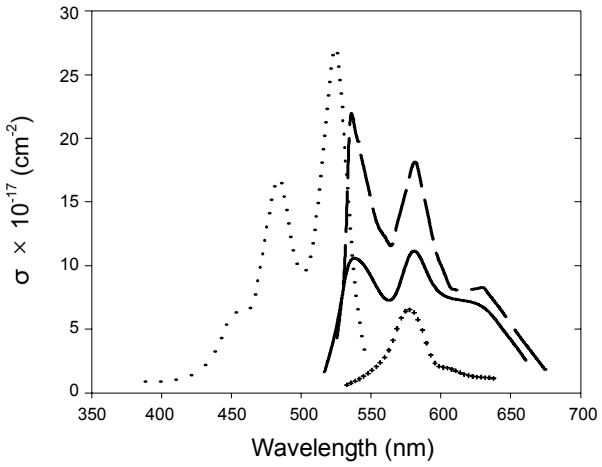

Figure 1. Electronic absorption spectrum (···), emission Spectrum (---), excited state absorption spectrum (—) and (xxx) ASE spectrum of DBPI in DMF.

Cyclic voltammetry measurements were made using a conventional three electrode cell configuration linked to an EG & G model 170 PAR apparatus. The platinum electrode surface was 1×10^{-6} m^2 as a working electrode, coiled platinum wire as a counter electrode, saturated Ag/AgCl as a reference electrode. The potential was calculated with relative to the Ag/AgCl reference electrode whose potential is at about 0.200 V versus SHE at 25 °C. and 0.1 mol/L tetrabutyl ammonium perchlorate (TBAP) as background electrolyte. Cyclic voltammograms were recorded after background subtraction and iR compensation to minimize double-layer charging current and solution resistance.

The working electrode was polished on a polisher Ecomet grinder. Cyclic voltammetric data were obtained at scan rate ranging from 0.02 to 2 *V/s* in non aqueous media at (22 ± 2) °C. Digital simulation of the data for cyclic voltammetric experiments was carried out on a PC computer using EG & G condesim package. Convolution-deconvolution transforms was performed using EG & G condecon software package. All working solutions were throughly degassed with oxygen free nitrogen and a nitrogen atmosphere was maintained above the solution throughout the experiments.

Results and Discussion

Spectral behavior of DBPI. 5×10^{-4} M of DBPI in DMF give amplified spontaneous emission (ASE) with maximum at 580 nm upon excitation by nitrogen laser (λ_{ex} = 337.1 nm). The ground state absorption cross section (σ_A), the emission cross section (σ_E) as well as effective emission cross section is shown in Fig. 1. The excited state absorption cross section (σ^*_A) is given from the difference ($\sigma_E - \sigma^*_E$). We interpret this difference as the first excited singlet state absorption band which reduces the dye laser efficiency. The low intensity of amplified spontaneous emission (ASE) could be interpreted to the $s_1 \rightarrow s_n$ transition and reabsorption of emitted photons by ground state molecules due to the strong overlap between emission and absorption spectra (overlap area was calculated as 8.6×10^{-13}

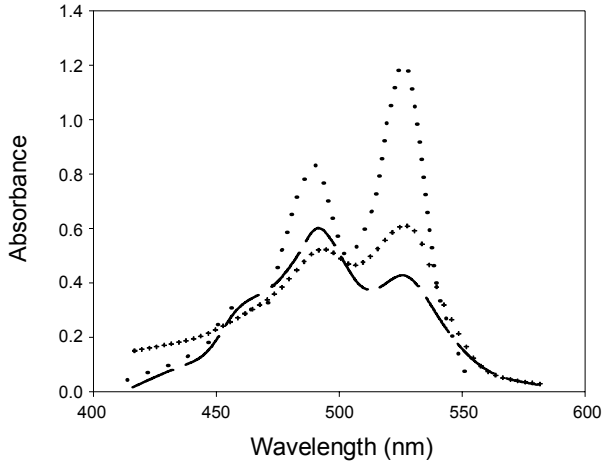

Figure 2. Absorption spectra of 1×10^{-5} M of DBPI in (···) ethanol, (xxx) 1 N NaOH ethanolic solution and (---) 50 % aqueous ethanol.

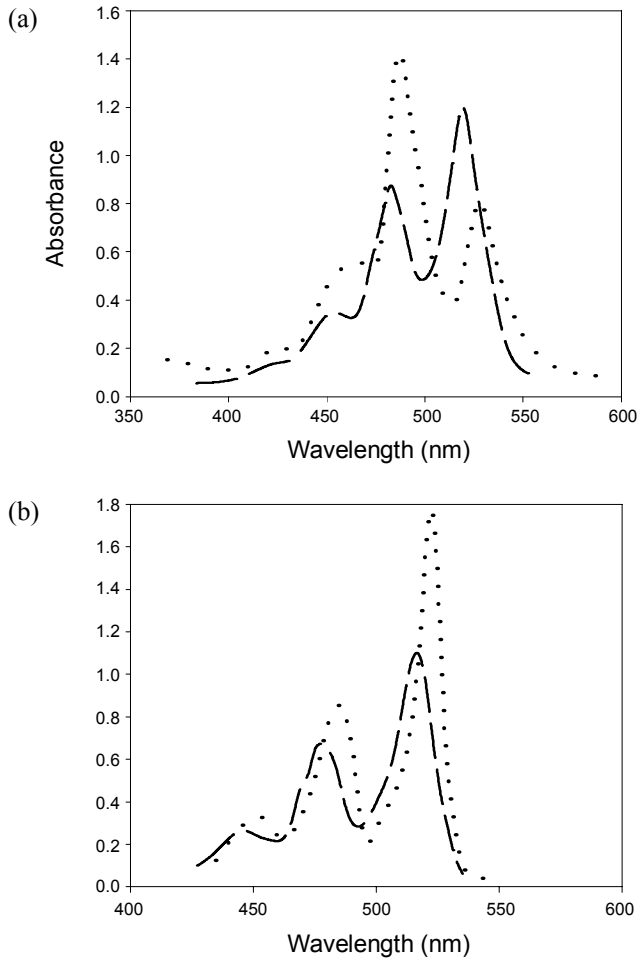

Figure 3. Absorption spectra of 1×10^{-5} M DBPI in (a) ethanol and (b) in THF at (---) 300 k and (···) 77 K.

mol dm^{-3} cm^3 from the relation.[21-24]

$$J = \int \varepsilon(\acute{\upsilon})\, f(\acute{\upsilon})\, \acute{\upsilon}^{-4}\, d\acute{\upsilon} \quad (6)$$

Where f (ύ) is the emission intensity normalized to unity and ε (ύ) is the molar absorptivity of DBPI in DMF. The populations of DBPI triplet state *via* intersystem crossing also play a role in decreasing the intensity of ASE, the triplet state energy and lifetime of DBPI were 27.5 ± 2 kcal.mol^{-1} and 100 μs,[11] whears the energy and lifetime of excited singlet state are 54 kcal mol^{-1} and 3.7 ns. The photophysical properties of DBPI in solution are probably representative of perylene diimides in general. The high fluorescence quantum yield (ϕ_f = 0.96) and low triplet state energy of perylene diimides make them more likely to be useful as photosensitizer *via* the singlet rather than triplet excited state. On other hand, the fact that the triplet state is low-laying in energy but readily quenched by oxygen molecule[11] make these dyes useful as energy traps in antennae systems for photosensitizer generation of singlet oxygen.

The electronic absorption spectrum of 1×10^{-5} M of DBPI was measured in ethanol, 1 N sodium hydroxide ethanolic solution and 50% aqueous ethanol. As shown in Fig. 2, the spectral pattern of DBPI changes upon addition of sodium hydroxide and water to ethanol. It seems that the addition of water and sodium hydroxide favors the aggregation of DBPI dye and the tendency of dye to aggregate is higher in polar solvent. The spectral changes shown in Fig. 2, (the extinction coefficients were reduced, the bands were red shifted and broadened and relative intensities of maximum were shifted to highest energy band near 485 nm). These differences are indicative of the presence of aggregates higher than dimmer. The aggregation also occurs in frozen sample (at 77 K) in ethanol at concentration of 1×10^{-5} M but it is not in tetrahydrofuran (THF) as shown in Fig. 3. This indicates that the polarity of solvent plays more important role in enhancing the aggregation of DBPI dye. It seems that the electrostatic repulsion between DBPI dye molecules decreases in polar solvents.

Study of contact ion pair. A compound formed when a cation and a negative ion interact with each other by coulomb attraction to get close together, but with both charges still separated, is called a contact ion pair. Since the charge separation is complete, a large dipole moment can be expected. The formation of a contact ion pair usually occurs by electron transfer from excited donor to the acceptor. In order for such a compound to be formed a low ionization potential of the donor and high electron affinity of acceptor are necessary. A direct observation of a contact ion pair $DBPI^{+}Cl^{-}$ in CCl_4 solvent was studied by UV-visible absorption technique. Photoirradiation of 8×10^{-6} M of DBPI by 525 nm light ($I_o = 5 \times 10^{-6}$ Ein/min) in CCl_4 (E_A = 2.12 eV) causes a decrease in absorbance and a new absorption peak appears at 570 nm with isobestic point at 540 nm (Fig. 4). The photochemical quantum yield (ϕ_c) of ion pair formation was calculated using a method described elsewhere[25] and was found to be ϕ_c = 0.018, the formation of ion pair is a one photon process as represented by reaction 7 and 8.

$$DBPI + h\upsilon \rightarrow DBPI^* \quad (7)$$

$$DBPI^* + CCl_4 \rightarrow DBPI^{+}Cl^{-} + {}^{\cdot}CCl_3 \quad (8)$$

We propose that the electron transfer from the excited singlet state of DBPI to CCl_4 in the transient excited charge transfer complex is the main primary photochemical process which

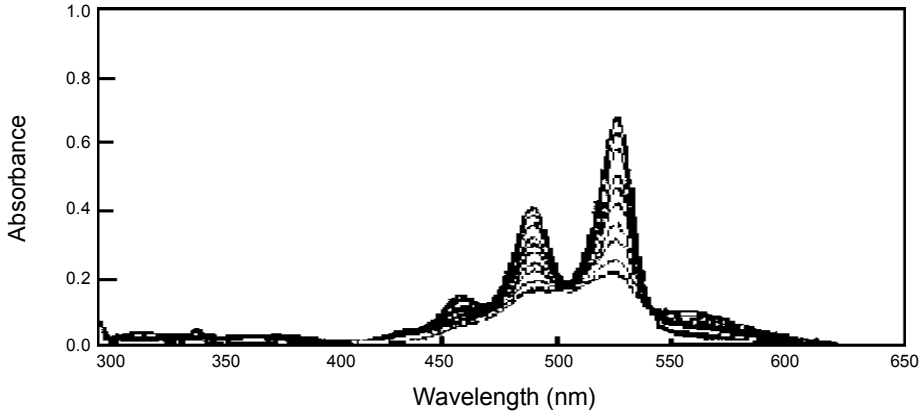

Figure 4. Effect of irradiation on the electronic absorption spectrum of 8×10^{-6} M of DBPI in CCl_4 (λ_{irr} = 525 nm) the irradiation times at decreasing absorbance are 0.0, 5, 9, 16, 30, 40, 65, 75, 100 and 125 min.

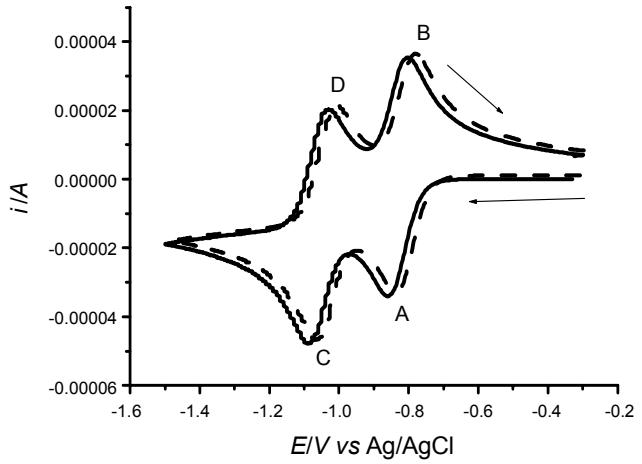

Figure 5. Reductive cyclic voltammogram of 2.5×10^{-3} *M* of DBPI in CH_3CN/0.1 M TBAP (------) and in DMF/0.1 M TBAP (——) at scan rate of 0.5 *V/s*.

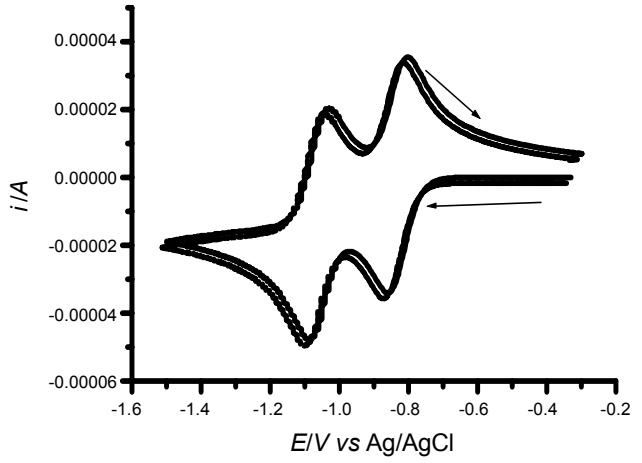

Figure 6. Matching between reductive experimental voltammogram of DBPI dye (——) and simulated voltammogram (·····) at a sweep rate of 0.5 *V/s*.

initiates a chemical reaction. It leads to the radical cation, a chloride ion and a trichloromethyl radical in solvent cage. The photoionozation of some aromatic and aliphatic amines in chloromethane solvents has been reported.[26,27] Photoreactivity of some anthracene and perylene derivatives are recently reported.[28-31]

Electrochemical studies of DBPI.

Cathodic electroreduction process: Cyclic voltammetric studies – Cyclic voltammetry of the reductive process of 2.5×10^{-3} mol/L of the DBPI dye compound was measured in two solvents, 0.1 mol/L TBAP/CH_3CN and 0.1 mol/l TBAP/DMF at scan rates ranging from 0.02 - 5 *V/s*. In both solvents, the first reductive peak (A) was coupled with the oxidative peak (B) while the second reductive peak (C) was coupled with the oxidative peak (D). It was found that the first and the second peak currents increased with scan rate, while the forward and the reverse peak potentials of the first and the second reduction processes in CH_3CN solvent were independent on the scan rate. The constancy of peak separation (ΔE_p = 59 mV) with variation of scan rate gives evidence that, the first and the second reduction processes of the investigated laser dye proceed as fast charge transfer at all sweep rates.[32] This behaviour demonstrates that the first charge transfer produces a radical anion that gains another electron to form a dianion. Fig. 5 gives an example of the cyclic voltammograms at sweep rate of 0.5 *V/s* of the DBPI dye in 0.1 mol/L TBAP/DMF and 0.1 mol/L TBAP/CH_3CN solvents. It was observed that the redox potentials (E^0_1 & E^0_2) of DBPI dye shifted slightly to more negative potential in the case of DMF than CH_3CN. This behaviour demonstrates more stabilization of DBPI in DMF than CH_3CN and the activation energy barrier in case of DMF is higher than that in case of CH_3CN. The ratio of the anodic to cathodic peak current demonstrates the rapidity of the charge transfer.

In CH_3CN the measured values of peak width of two waves, $E_p - E_{p/2} = 56.5/n$ mV ± 2 mV, demonstrate the reversibility behaviour of the investigated system, where E_p, $E_{p/2}$ and n are the peak potential, the half-peak potential and the number of electrons respectively.

The peak separation ΔE_p of the first charge transfers was found to be 60 mV in the case of CH_3CN and DMF while for

Table 1. Electrochemical parameters of the cathodic reduction process of DBPI dye

	Electrochemical Parameters						
Solvent	$-E^0_1$ V	$-E^0_2$ V	$k_{s1} \times 10^3$ m s^{-1}	$k_{s2} \times 10^3$ m s^{-1}	$D_1 \times 10^9$ m^2 s^{-1}	$D_2 \times 10^9$ m^2 s^{-1}	α
CH_3CN	0.810[a]	1.055	2.50	3.10	3.50	3.85	0.48
	0.812[b]	1.056	2.60	3.30	3.60	3.79	0.49
	—[c]	—	—	—	3.46	3.46	—
	0.813[d]	1.055	—	—	3.23	3.54	—
	—[e]	—	—	—	3.90	3.41	—
DMF	0.850[a]	1.140	1.80	2.50	2.23	2.72	0.45
	0.853[b]	1.142	1.91	2.70	2.72	2.81	0.46
	—[c]	—	—	—	2.93	2.65	—
	0.855[d]	1.144	—	—	2.22	2.74	—
	—[e]	—	—	—	2.53	2.82	—

[a]Experimental values. [b]Simulated values. [c]Values of *D* calculated *via* Eq. (15). [d]Values calculated from convolutive voltammetry. [e]Cottrel plot.

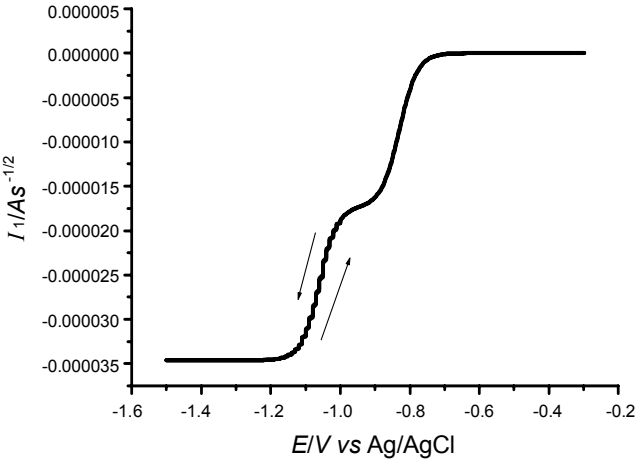

Figure 7. Convolution voltammetry (I_1) of the reductive process of *DBPI* dye at sweep rate of 0.2 *V/s*.

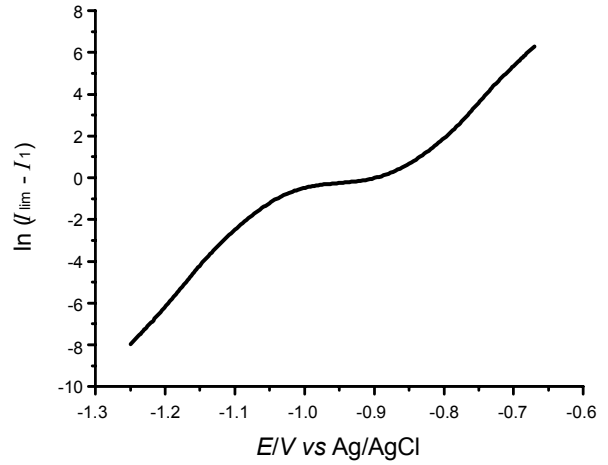

Figure 8. plot of $ln(I_{lim} - I_1) / I_1$ versus E of the reductive waves at sweep rate of 0.2 *V/s* of the *DBPI* dye.

the second peak is 60 mV in case of CH_3CN and 75 mV in case of DMF confirming the rapidity of charge transfer in 0.1 mol/L TBAP/CH_3CN, while in case of 0.1 mol/L TBAP/DMF it was found that the reversibility of the first charge transfer and the quasireversibilty of the second charge transfer. The redox potential (E^o) was determined from the mean position of the peak potentials (Table 1). Based on the above discussion the given redox reaction might be confirmed as reversible faradaic processes. The standard heterogeneous rate constant (k_s) was determined from the generated cyclic voltammograms.[32] From the plot of i_p *vs.* $\sqrt{v}$, the diffusion coefficient (D) of the electroactive species is determined.[32,33] The calculated values of D are cited in Table 1. As it was expected,[34] the diffusion coefficient of DBPI decreases in the order CH_3CN > DMF, due to the increase of the viscosity of the solvent medium on going from CH_3CN to DMF. The decrease of the solvent viscocity indicates that the diffusion of DBPI follows the chemical Stokes-Einstein relation.[34] The results given in Fig. 6 employ the experimental and theoretical values of the electrochemical parameters of the DBPI dye, which demonstrate excellent agreement between the captured and the simulated data.

Convolution transforms – In cases of straight forward electron transfer or subsequent chemical reaction, the I_1 convolution which is defined as:[35-38]

$$I_1 = (1/\sqrt{\pi})\int_0^t \frac{i(u)}{\sqrt{(t-u)}}\,du \qquad (9)$$

allows to determine the diffusion coefficient of the bulk species from the Eq. (10):[35]

$$I_{lim} = nFAC\sqrt{D} \qquad (10)$$

where I_{lim} is the limiting value achieved for I_1 when the potential is driven to a sufficiently extreme value past the wave; the other terms have their usual significance.

The values of the diffusion coefficient (D) corresponding to the reduction step were calculated *via* Eq. (10) and are listed in Table 1. The I_1 convolution of the reductive voltammogram of DBPI at a scan rate of 0.2 *V/s* is indicated in Fig. 7. The I_1 convolution of the backward sweep are completely overlay on the forward one and return to zero, confirming the simple elec-

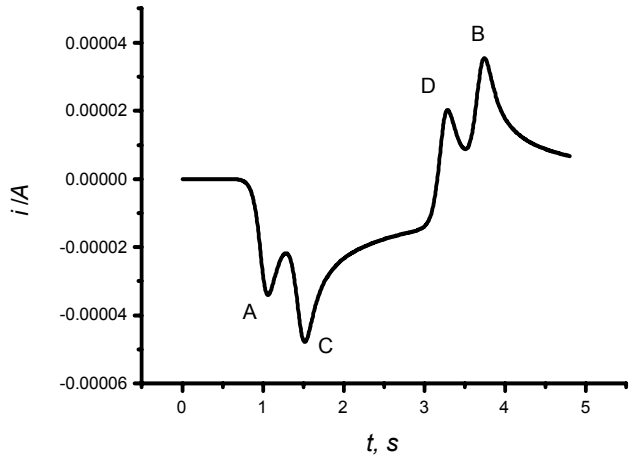

Figure 9. Plot of *i* versus *t* corresponding to a reductive cyclic voltammogram at sweep rate of 0.5 *V/s*. The point $t = 2.5$ s is the time at which the potential scan is switched to the reverse direction.

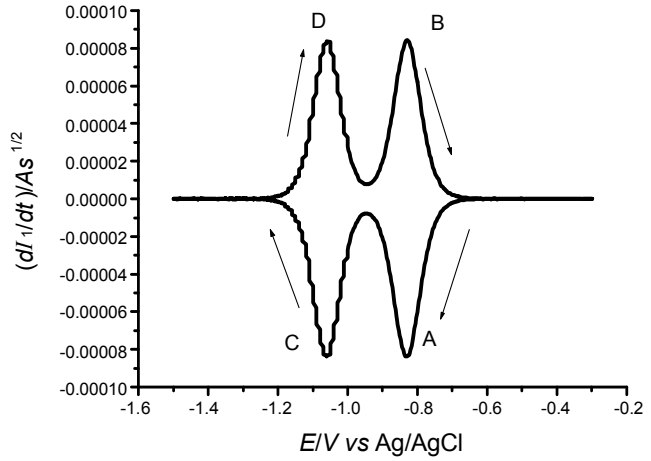

Figure 10. Deconvolution voltammetry (dI_1/dt) of the reductive cyclic voltammogram of DBPI at sweep rate of 0.2 *V/s*.

tron transfer and the rapidity of the two charge transfer between the electrode and the electroactive dye compound DBPI, *i.e fast EE* mechanism.

In the case of fast electron transfer, the following equation is applied:[39]

$$E = E_{1/2} + RT/nF \ln (I_{lim} - I_1) / I_1 \quad (11)$$

The plot of $\ln (I_{lim} - I_1) / I_1$ versus E should be linear with a slope of reciprocal of nF/RT for a simple electrode process. Fig. 8 shows the plot of $\ln (I_{lim} - I_1) / I_1$ versus E which exhibits two slope lines for the two consecutive charge transfer with slope = 1/0.025 for each line, confirming the rapidity of both charge transfer and also provide overall n value equals to two.

The presentation of *i vs t* of the voltammogram at sweep rate 0.2 *V/s* is shown in Fig. 9. The plot produces discontinuity Δi_c at t = 2.5 s due the reversibility of the scan. By selecting the data points a cottrel plot is obtained as current versus the reciprocal square root of time. The slope of Cottrel plot yields a diffusion coefficient $D = 4.2 \times 10^{-9}$ m^2 /s. Inspection of Fig. 9 revealed that, the height of the forward and reverse peaks are the same, i.e the height of peak A is equalled to the height of peak B and the height of peak C is equalled to the height of peak D confirming the rapidity of the simple charge transfer processes of DBPI dye.

Deconvolution transforms – The deconvolution transforms of the current ($d I_1 /dt$) as a function of E of reversible process is defined as:[40]

$$e_p = (dI_1/dt) = nFAC\sqrt{D}\, a\zeta / (1+\zeta)^2 \quad (12)$$

where $a = nvF/RT$ (13)

and $\zeta = exp\,[nF/RT\,(E - E^0)]$ (14)

and the representation of this equation at $v = 0.2$ *V/s* in 0.1 M TBAP/CH_3CN is indicated in Fig. 10. The width of deconvoluted peak w^p at half peak height of two deconvoluted current equals to 3.53 RT/nF = 90.5 /n mV for fast charge transfer. It was found that $w^p = 90 \pm 2$ mV for both peaks , confirming the rapidity of both charge transfer.

The symmetry and alignment of the forward and reverse sweep, further confirming the rapidity of both charge transfer of the reduction process of DBPI dye. The standard reduction potential was determined from the deconvoluted peak current of the two peaks (Table 1). The values of E^0_1 and E^0_2 determined from deconvolution voltammetry *via* Figure 10 compare well with the values calculated from cyclic voltammetry (Table 1). The peak height for fast electron transfer is predicted to proportional to the concentration of the reducible species, to the electrode surface area and to the scan rate v. The peak potential for reversible process is a constant equal to the polarographic half wave potential. The peak shape is very dependent on n, the number of transferred electrons, as n increase, the peak is predicted to become narrower and much higher. It was found that, the I_1 *vs* E and (dI_1/dt) *vs* E curves were easier to interpret more than *i vs E* curve.

Also, the values of diffusion coefficient were calculated from deduced convoluted current (I_{limd}) *via* the following relationship:[32,35]

$$I_{limd} = \frac{i_{prev}}{2.788\sqrt{(nv)}} \quad (15)$$

where I_{limd} is the deduced limiting convoluted current, which is defined as the limiting convoluted current. The value of diffusion coefficient calculated from I_{limd} agrees well with the value calculated from cyclic voltammetry and convolutive voltammetry of the experimental voltammogram (Table 1).

Also, the number of electrons consumed in electrode reaction can be calculated from the following equation:[32]

$$n = 0.103\, ep/\, v\, I_{limd} \quad (16)$$

which is found to be equalled to 2 for the overall reduction process.

From the obtained result, it can be seen that the redox poten-

Table 2. Electrochemical parameters of the oxidation process of DBPI dye

	Electrochemical Parameters								
Solvent	E^0_1 V	E^0_2 V	$k_{s1(dimer)} \times 10^4$ m s^{-1}	$k_{s2(dimer)} \times 10^4$ m s^{-1}	$D_1 \times 10^9$ m^2 s^{-1}	$D_2 \times 10^9$ m^2 s^{-1}	k_{dim1} s^{-1}	k_{dim2} s^{-1}	α
CH_3CN	1.315[a]	1.550	7.53	8.40	4.5	4.7	—	—	0.49
	1.317[b]	1.552	7.50	8.31	4.6	4.8	7.6	14.4	0.49
	—[c]	—	—	—	4.5	4.4	—	—	—
	1.316[d]	1.553	—	—	4.6	4.5	—	—	—
	—[e]	—	—	—	5.20	5.80	—	—	—
DMF	1.357[a]	1.592	6.81	7.53	3.97	3.62	—	—	0.43
	1.356[b]	1.590	6.92	7.45	3.61	3.23	7.5	14.7	0.44
	—[c]	—	—	—	3.13	3.24	—	—	—
	1.355[d]	1.591	—	—	3.62	3.19	—	—	—
	—[e]	—	—	—	3.61	2.75	—	—	—

[a]Experimental values. [b]Simulated values. [c]Values of *D* calculated *via* Eq. (19). [d]Values calculated from convolutive voltammetry. [e]Cottrel plot.

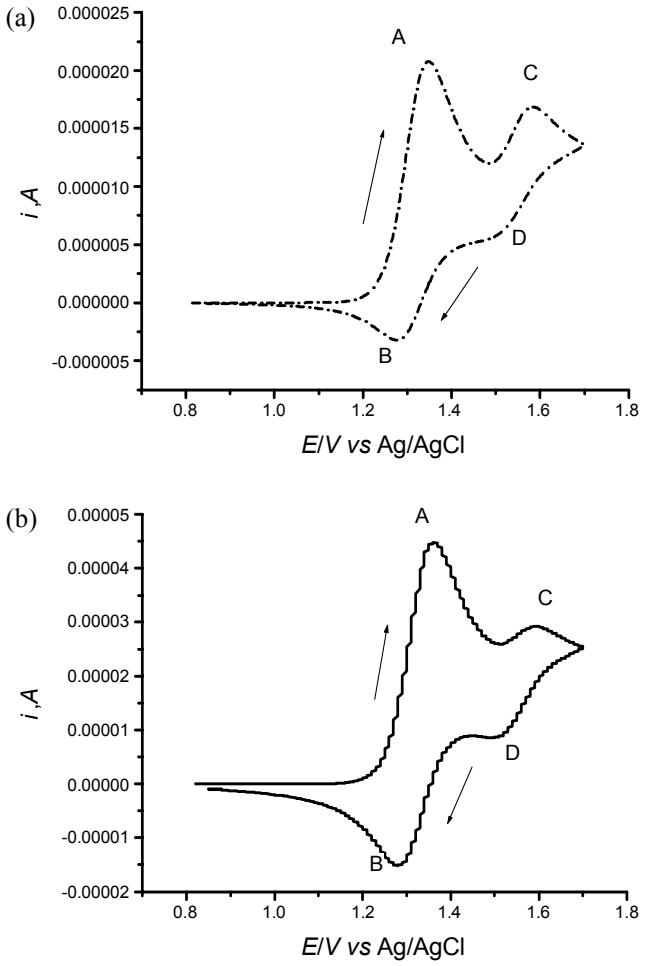

Figure 11. Oxidative cyclic voltammograms of *DBPI* in CH_3CN (a) at scan rate of 0.2 *V/s* and (b) at scan rate of 0.5 *V/s*.

tial of the second reduction process is more negative than that of the first one, which indicates that the second process requires more energy than the first one. As the degree of interaction increases, ΔE^o and K_c also increase. The separation of the peak potentials for systems with two redox centers is in terms of the comproportionation equilibrium constant of the intermediate (*i.e* the product of the first electron transfer reaction). This is given by the following equation:[38]

$$K_c = \exp\left[\frac{(E^0_1 - E^0_2)\,F}{RT}\right] \quad (17)$$

which gives 3.16×10^9 for K_c value, indicating extensive delocalization of charge between the centers of DBPI dye ($K_c > 10^6$).[41]

Anodic electrooxidation of DBPI dye:

Cyclic voltammetric behaviour− The electrooxidation of dye compound DBPI exhibited two oxidative peaks. The first oxidative peak (A) is coupled with one reductive peak (B) at all sweep rates (0.02 - 5 *V/s*), while the second oxidative peak (C) is coupled with one reductive peak (D) which appears only at sweep rate higher than 0.2 *V/s*. An example response of the oxidative cyclic voltammogram of DBPI dye at sweep rates of 0.2 and 0.5 *V/s* is illustrated in Fig. 11. As indicated, for the first oxidative peak (A & B) the ratio of i_{pc}/i_{pa} is less than 1.0 at all sweep rates, while for the second one (C) the coupled reductive peak (D) appears only at sweep rate > 0.5 *V/s* with ratios of i_{pc}/i_{pa} less than one, indicating the $EC_{dim1}\,EC_{dim2}$ mechanism for both oxidative processes. The appearance of second coupled peak (D) at higher sweep rate confirms the presence of a fast dimerization process after the second charge transfer. In addition, the ratio of the peak currents i_{pc}/i_{pa}, increases with increasing scan rate. Furthermore, the current function of this cathodic peaks, $i_{pc}/\sqrt{v}$, decreases slightly with scan rate. According to these results the underlying process is expected to be EC mechanism i.e., electron transfer is followed by chemical reaction.[34] The accompanying reaction might be a dimerization reaction which occurs between the initial DBPI and the monocation product moieties in the first step (EC_1) while in the second step it occurs between the initial DBPI and the dication product moieties. Also the shift of both peak potentials (A & B) and (C

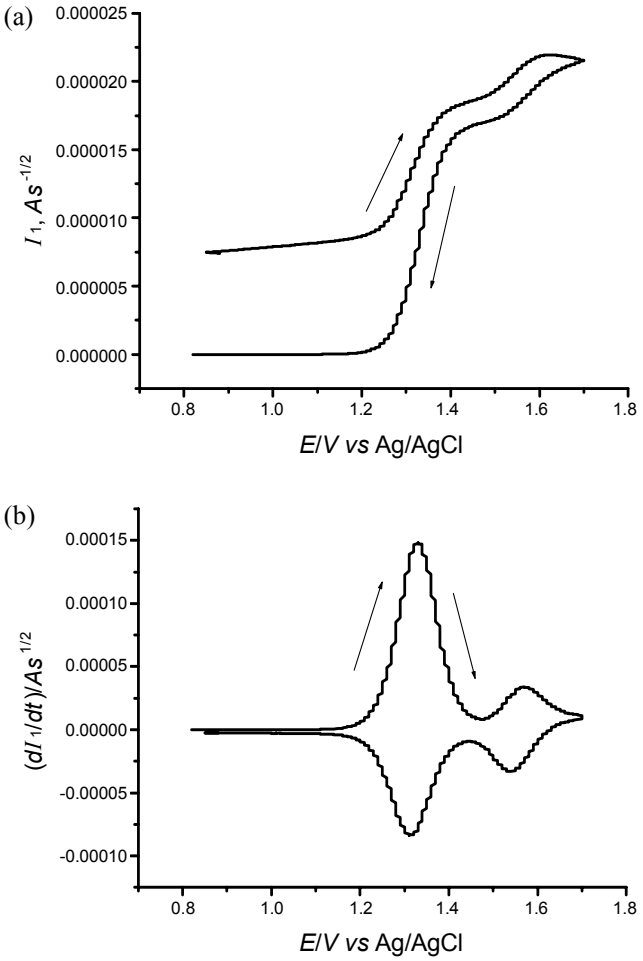

Figure 12. (a) I_1 convolution transforms of oxidation process of DBPI dye at sweep rate of 0.2 *V/s*. (b) (dI_1/dt) deconvolution transforms of oxidation process of DBPI dye at sweep rate of 0.2 *V/s*.

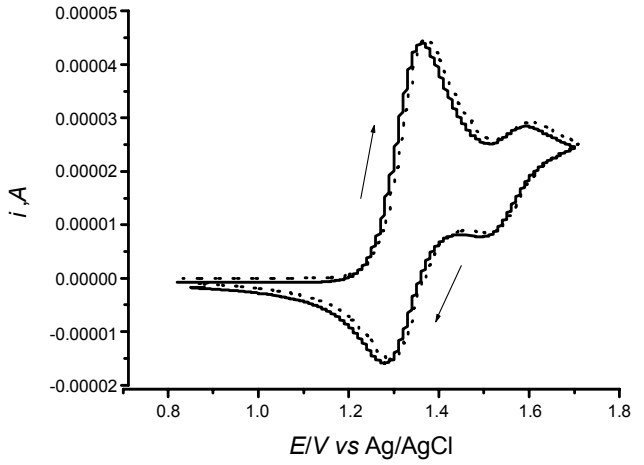

Figure 13. Matching between oxidative experimental voltammogram of *DBPI* dye (——) and simulated voltammogram (·····) at a sweep rate of 0.2 *V/s*.

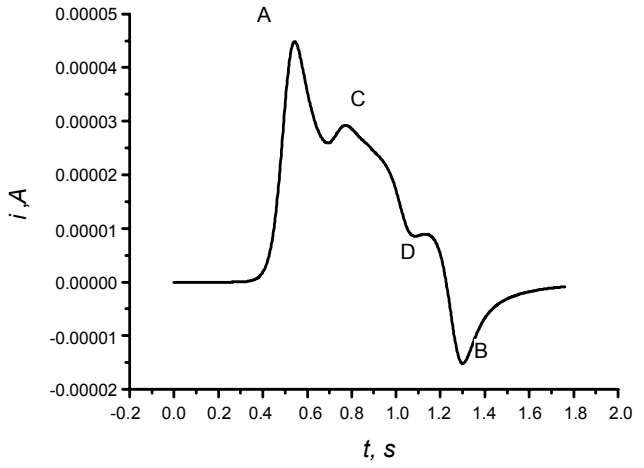

Figure 14. Plot of i versus t corresponding to oxidative cyclic voltammogram at sweep rate of 0.5 *V/s*. The point $t = 0.99$ s is the time at which the potential scan is switched to the reverse direction.

& D) to more positive values with increasing the sweep rates reflect the deviation of both charge transfer from the nernstian behaviour.

It was established that, the electrooxidation of perylene diimide multichromophores in CH_2Cl_2 yields one oxidative wave is followed by dimerization reaction which takes place in the para position of the outer phenyl ring.[42-44] This behaviour supports and confirms our oxidative electrochemical properties of the investigated DBPI compound in this article.

The redox potentials (E^0_1 & E^0_2) of DBPI dye were calculated from the average peak position and were listed in Table 2. It was observed that the values of E^0_1 & E^0_2 in case of using DMF is more positive than that in case of CH_3CN. This behavior attributed to increasing the polarization effect of DMF causing the difficulty of charge transfer. The H-bond cooperativity of cations or multiple H-bonds can be described as a polarization effect of the lone pairs of the bonding XH groups by van der Waals interactions. Also the variation of the redox potential (E^o) of the DBPI/DBPI$^+$ couple might analyzed in terms of the electron-accepting power of the solvent medium. Hence, the E^o of the DBPI/DBPI$^+$ and DBPI$^+$ / DBPI^{++} couples shifted to more positive values in weak electron-acceptor solvent such as DMF and tended to become less positive in strong electron-acceptor solvent such as CH_3CN.[45]

The standard heterogeneous rate constant ($k_{s(dimer)}$) was determined from the working curve (7.53×10^{-4} m/s)[32] and from digital simulation by the good agreement between the experimental and theoretical voltammograms. Also, the diffusion coefficient was determined from the slope of i_p *vs* $\sqrt{v}$.[34,37] The symmetry coefficient (α) of the oxidative processes cited in Table 2 was calculated from the values of half-peak width of the cyclic voltammograms *via* the following equation:[46]

$$E_p - E_{p/2} = 48/\alpha n_a \quad (18)$$

As shown from Table 2 the values of α are slightly less than 0.5 which reflect that the activation energy for the oxidation process is increased by small magnitude aside from the effect

of potential difference between the electrode and the solution.

Convolution-deconvolution transforms: In the case of moderate fast electron transfer, the diffusion coefficients (*D*) of the DBPI dye compound under investigation was determined from the following deduced limiting convoluted current equation:[32,35]

$$I_{limd} = i_p / 3.099(/ \alpha n_a v)^{1/2} \quad (19)$$

The calculated values of the diffusion coefficient (D) are listed in Table 2. Fig. 12 exhibits the I_1 convolution and deconvolution transforms of the oxidative process at 0.2 *V/s* indicating the quasireversibility of charge transfer process and confirm the presence of dimerization process following the two charge transfer[42-44] i.e EC_{dim1} EC_{dim2} mechanism. The values of standard reduction potentials (E^0_1 & E^0_2) were determined from the average peak position of the deconvoluted voltammograms (Table 2).

Also the homogeneous chemical rate constants of the dimerization process (k_{dim}) were calculated from digital simulation methode and cited in Table 2.

Fig. 13 shows an example of the comparison between the oxidative experimental and the theoretical voltammograms of DBPI dye at sweep rate of 0.5 *V/s*, which indicates well agreement between the two curves confirming the accuracy of the electrochemical parameters obtained from experimental cyclic voltammograms. The oxidative experimental and theoretical data of DBPI were listed in Table 2.

The presentation of *i vs t* of the oxidative anodic voltammogram at sweep rate of 0.5 *V/s* is shown in Fig. 14. The plot produces discontinuity Δi_c at t = 0.99 s due the reversibility of the scan. Inspection of Fig. 14 revealed that, the inequality of the height of the forward and backward peaks, i.e the height of peak A is unequal to the height of peak B and the height of peak C is unequal to the height of peak D confirming that both charge transfer are followed by a chemical processes which may be attributed to the aggregation of the mono cation radical $DBPI^+$ with the initial dye molecule DBPI due to the columbic attraction force which is represented in the simple form as $DBPI^+$ …. DBPI i.e $(DBPI)_2^+$ of the first chemical process and the aggregation of dication $DBPI^{++}$ with the initial dye DBPI as $DBPI^{++}$. ..DBPI i.e.. $(DBPI)_2^{++}$ of the second step. Also, the extended л-systems of DBPI forms cause an high aggregation tendency forming dimeric and/or oligomeric species.

By selecting the data points a cottrel plot is obtained as current versus the reciprocal square root of time. The slope of Cottrel plot yields a diffusion coefficient $D = 5.2 \times 10^{-9}$ m^2 /s.

It was observed that, the redox potential of the second reduction process is more positive than that of the first one, which indicates that the second process requires more energy than the first one. From the value of ΔE^o, the K_c value was calculated using Eq. 17 and found to be 1.415×10^9 indicating extensive delocalization of charge between the centers of DBPI dye ($Kc > 10^6$).[42]

From the above electrochemical studies the reductive and oxidative electrode behavior of DBPI dye can be proposed to proceed as follows:

Reductive process.

$$[DBPI] + e \leftrightarrow [DBPI]^- + e \leftrightarrow [\ DBPI]^-$$ i.e. EE mechanism

Oxidative process.

$$[DBPI\ ] - e \leftrightarrow [DBPI]^{+} - e \leftrightarrow [DBPI]^{++}$$

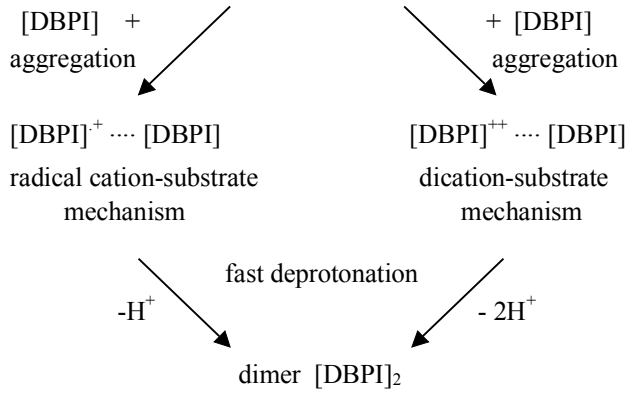

i.e. $EC_{dim1}EC_{dim2}$ mechanism

Conclusion

It can be concluded that DBPI gives amplified spontaneous emission in DMF with maximum at 580 nm upon excitation with nitrogen laser and displays molecular aggregation in water at room temperature and in EtOH at low temperature, the presence of NaOH in ethanolic solution favor the molecular aggregation. The DBPI displays photodecomposition in carbon tetrachloride upon irradiation with 525 nm light. The electrochemical behavior of cathodic reduction of DBPI dye in 0.1 M TBAP/CH_3CN and 0.1 M TBAP/DMF at a platinum electrode takes place as two reduction peaks (A & B) and (C & D). This behavior demonstrates that the first charge transfer produces a radical anion that gains another electron to form a dianion. The redox potentials of the investigated dye compound shift to more negative potential in the case of DMF, indicating that more stabilization of DBPI dye in DMF than in CH_3CN.

Electrooxidation of DBPI dye gave two anodic oxidation peaks, the second one at low sweep rate ≤ 0.5 *V/s* behaves as unidirectional irreversible peak. The experimental kinetic parameters were determined experimentally and verified *via* a digital simulation method by comparing the generated theoretical voltammograms with the experimental voltammograms. The oxidative electrode reaction proceed as $EC_{dim1}EC_{dim2}$. The chemical processes were attributed to the dimerization of the initial neutral molecules with the monocations in the first step and with the dication species in the second step.

Acknowledgments. We thank Kyoto Institute of Technology for lifetime and low temperature measurements.

References

1. Luckac, I.; Langhals, H. *Chem. Ber.* **1983**, *116*, 3524.

2. Ford, W. E. *J. Chem*. **1986**, *34*, 43; **1987**, *37*, 189.
3. Balzani, V.; Bolletta, F.; Scandola, F.; Ballardini, R. *Pur. Appl. Chem*. **1975**, *51*, 299.
4. Darwent, J. R.; Douglas, P.; Harriman, A.; Rickoux, G. M. C. *Coord. Chem. Rev*. **1982**, *44*, 83.
5. Kavarnos, G. J.; Turro, N. J. *Chem. Rev*. **1986**, *86*, 401.
6. Aubert, C.; Funfshiling, J.; Granacher, I. Z.; Langhals, H. *Anal. Chem*. **1985**, *320*, 361.
7. Sandra, M.; Bird, G. R. *Opt. Commun*. **1984**, *851*, 62.
8. Wasielewski, M. R.; Niemczyk, M. P.; Svec, W. A.; Pewitt, E. B. *J. Am. Chem. Soc*. **1985**, *107*, 5562.
9. Rademacher, A.; Markle, S.; Langhals, H. *Chem. Ber*. **1982**, *115*, 2927.
10. Langhals, H. *Chem. Ber*. **1985**, *118*, 4641.
11. Ford, W. E.; Komot, P. V. *J. Phys. Chem*. **1987**, *91*, 6373.
12. Ebeid, E. M.; El-Daly, S. A.; Langhals, H. *J. Phys. Chem*. **1988**, *92*, 4565.
13. El-Daly, S. A. *J. Photochem & Photobiol, A: Chem*. **1992**, *68*, 51.
14. El-Daly, S. A.; Okamoto, M.; Hirayama, S. *J. Photochem& Photobiol. A: Chem*. **1995**, *91*, 105.
15. El-Daly, S. A.; Hirayama, S. *J. Photochem. & Photobiol. A: Chem*. **1997**, *110*, 59.
16. El-Daly, S. A. *Montshefite fur Chemie* **1998**, *129*, 835.
17. Demas, J. N. *Excited state lifetime measurements*; *Academic Press*: New York, 1993; Chap. 6.
18. Klink, M. Ph. D. Thesis, University of Konstanz, 1995.
19. Hatchard, C. G.; Parker, C. A. *Proc. Ray. Soc*. **1965**, *A 235*, 518.
20. Steven Murov, L. *Hand book of Photochemistry*; Marcel Dekker INC: New York, 1973; Sec. 13.
21. Greef, R.; Peat, R.; Peter, L. M.; Pletcher, D.; Robinson, J. *Instrumental Method in Electrochemistry*; *John Wiley and Sons*: New York, 1985; Chap. 6.
22. Kissinger, P. T.; Heineman, W. R. *J. Chem. Edu*. **1983**, *60*, 703.
23. Polcyn, D. S.; Shain, I. *Anal. Chem*. **1966**, *38*, 371.
24. Langhals, H.; Karolin, J.; Johansson, L. B. *J. Chem. Soc. Faraday Trans*. **1998**, *91*, 2919.
25. Ebeid, E. M.; Issa, R. M.; Ghoneim, M. M.; El-Daly, S. A. *J. Chem. Soc. Faraday Trans*. **1986**, *1*, *82*, 909.
26. Bard, A. J.; Ledwith, A.; Shine, H. J. *Adv. Phys. Org. Chem*. **1971**, *21*, 155.
27. Shimamon H. In *Photochemistry and Photophysics*; Robek, J. F., Ed., CRC Press: New York, 1992; Vol. VI, Chap. 2, p 65.
28. Azim, S. A.; El-Daly, H. A.; El-Daly, S. A.; Abou-zeid, Kh. A.; Ebeid, E. M.; Heldt, J. R. *J. Chem. Soc. Faraday Trans*. **1996**, *92*, 2685.
29. El-Daly. S. A. *Spectrochimica Acta part*. **1999**, *A 55*, 143.
30. El-Daly, S. A.; Fayed, T. A. *J. Photochem. & Photobiol. A: Chem*. **2000**, *137*, 15.
31. El-Daly, S. A.; Awed, M. K.; Abdel-Halim, S. T.; Dowider, D. A. *Spectrochimica Acta part A*, In Press **2008**.
32. El-Daly, S. A.; El-Hallag, I. S.; Ebeid, E. M.; Ghoneim, M. M. *Chin. J. Chem*. **2009**, *27*, 241.
33. Nicholson, R. S.; Shain, I. *Anal. Chem*. **1965**, *37*, 722.
34. Tsierkezos, N. G. *J. Solution Chem.* **2007**, *36*, 1301
35. El-Hallag, I. S.; Ghoneim, M. M.; Hammam, E. *Anal. Chim. Acta* **2000**, *414*, 173.
36. Bard, A. J.; Faulkner, L. R. *Electrochemical Methods, Fundamentals and Applications*; Wiley: New York, 1980.
37. El-Hallag, I. S.; Hassanien. A. M. *Collect. Czech. Chem. Commun*. **1999**, *64*, 1953.
38. El-Hallag, I. S.; Ghoneim, M. M. *Monatsh. Chem*. **1999**, *130*, 525.
39. Ammar, F.; Saveant, J. M. *J. Electroanal. Chem*. **1973**, *47*, 215.
40. Catton, R. H.; Chisholm, M. H.; Huffman, J. C.; Lobkovsky, E. B. *J. Am. Chem. Soc.* **1991**, *113*, 8709.
41. Dalrymple-Alford, P.; Goto, M.; Oldham, K. B. *Anal. Chem*. **1977**, *47*, 1390.
42. Robin, M. B.; Day, P. Adv. *Inorg. Chem. Radioche*. **1967**, *10*, 247.
43. Cristina, F.; Ingo, O.; Tobias, S.; Eduard, F.; Gerd, S.; Michel, S.; Andreas, H.; Mark, van der A.; Frans C. de S.; Klaus, M.; Johan.; H. *J. Phys. Chem. C* **2007**, *111*(12), 4861.
44. Larumbe, D.; Moreno, M.; Gallardo, I.; Bertran, J.; Andrieux, C. P. *J. Chem. Soc., Perkin Trans*. **1991**, *2*, 1437.
45. Macdonald, J. R. *Physical review* **1953**, *92*, 4.
46. Marcoux, L. S.; Adams, R. N.; Feldberg, S. W. *J. Phys. Chem*. **1969**, *73*, 2611.